Proceedings of ESDA2004
7th Biennial ASME Conference on Engineering Systems Design and Analysis
July 19-22, 2004, Manchester, UK

ESDA2004-58398

NON-INTRUSIVE MEASUREMENT OF VOLUME AND MASS USING ELECTRICAL CAPACITANCE TOMOGRAPHY.

Andy Hunt
Tomoflow Ltd, Dorchester, United Kingdom
ahunt@tomoflow.com

John Pendleton
Tomoflow Ltd, Dorchester, United Kingdom
jpendleton@tomoflow.com

Malcolm Byars
Process Tomography Ltd, Wilmslow, United Kingdom
enquiries@tomography.com

Keywords: electrical capacitance tomography, ECT, mass measurement, dynamic weighing

ABSTRACT

Electrical capacitance tomography (ECT) has been used for some years to measure the concentration distribution within multiphase flows and processes. ECT is a relatively low resolution measurement, but it has many advantages, including being non-intrusive and fast. Recent developments of twin-plane systems have enabled measurements to be made of velocity as well as concentration. We have developed techniques to establish from these measurements the volume, mass and velocity of flow structures in two-component flows, and in particular the mass and velocity of large individual particles and groups of particles in solids/gas flow systems.

Results are presented in the paper for simple gravity-drop flows of partly-filled plastic spheres, plastic beads, and also for the conveying of granular material in a pilot plant. We show that resolution of mass to within a few grams is possible on objects of individual mass of between 2g and 35g. We also show measurements of flow structure volumes in vertical solids conveying pipes of approximately 50mm diameter. General comparisons are made with high-speed video photography of some of the flows, and the in the case of gravity-drop flows the accuracy of the mass measurement is established using weighing.

NOMENCLATURE

1,2 (as subscript), phase 1, phase 2
A, area
C, concentration
i (as subscript), zone I of n zones
k, the ratio K_H / K_L
K_{en}, mixture permittivity
K_H, relative permittivity of denser phase
K_L, relative permittivity of less dense phase
L_s, sensor electrode length
n, number of contiguous zones
q, volumetric flowrate
Q, volume
R, correlation coefficient
S, spacing (length) between electrode planes
t, time
T, averaging time
τ, delay time in correlation
V, velocity
x, concentration of dense phase in 2-phase mixture

INTRODUCTION

ECT measurements are made by placing rings of electrodes around the circumference of the pipe or vessel of interest, measuring the electrical capacitance between each independent pairing of electrodes and using image reconstruction techniques to show the permittivity distribution within the sensor. Sensor systems include sensor, capacitance measurement unit and control PC (Figure 1). Typical sensor arrangements have between 6 and 12 electrodes placed evenly on the circumference, with 5 or 6 rings of electrodes along the axial length – a total of between 30 and 60 electrodes each a few centimetres long. Usually rings 1, 3 and 5 or 1, 3, 4, and

6 are linked as guard electrodes, while rings 2 and 4 or 2 and 5 are the measurement sets. Figure 2 shows a typical electrode arrangement.

We have recently developed ECT systems that can make measurements at up to 300 complete frames of data per second for 6-electrode twin-plane systems [1]. A large range of sensor shapes and sizes may be fabricated but the most common are circular in cross section with diameters ranging from a few cm to some 10's of cm.

Estimating particle or structure volume from permittivity images requires calibration of permittivity to concentration, and a measure of velocity. Below we describe methods for achieving this.

CONCENTRATION MEASUREMENT BY ECT

ECT systems can be used to obtain images of the distribution of permittivity inside ECT sensors for any arbitrary mixture of different dielectric materials. One important application of ECT is viewing and measuring the spatial distribution of a mixture of two different dielectric materials (a two-phase mixture). From the permittivity distribution, we wish to obtain the distribution of the relative concentration (volume ratio) of the two components over the cross-section of the vessel. ECT is limited to flow systems where neither component is highly conducting, though some measurements are possible when the dispersed phase is slightly conductive, such as distilled water.

A typical ECT permittivity image format uses a square grid of 32 x 32 pixels to display the distribution of the normalised composite permittivity of each pixel. For a circular sensor, 812 pixels are used to approximate the cross-section of the sensor. The values of each pixel represent the normalised value of the effective permittivity of that pixel. In the case of a mixture of two dielectric materials, these permittivity values are related to the fraction of the higher permittivity material present at that pixel location.

The overall volume ratio of the materials inside the sensor at any moment in time is defined to be the percentage of the volume of the sensor occupied by the higher permittivity material. The volume of the sensor is the product of the cross-sectional area of the sensor and the length of the sensor measurement electrodes.

In the following analysis we refer to the relative permittivity (or dielectric constant) of materials. The relative permittivity of a material is its absolute permittivity divided by the permittivity of free space (or air). Hence the relative permittivity of air is 1 and typical values for other materials in solid or liquid format are polystyrene (2.5), glass (6.0) and mineral oil (2.3).

We have also used three different terms to describe the same concept, as they are all in common use. These are volume ratio, voidage and concentration, which we define to be the fraction of the higher permittivity material present in the mixture. These terms are inter-changeable.

ECT SYSTEM CALIBRATION PROCEDURE

In the normal method of operation, an ECT system is calibrated by filling the sensor with the two reference materials in turn and by measuring the resultant inter-electrode capacitance values at these two extreme values of relative permittivity.

This method of calibration defines the two end points of the measurement range for most types of ECT measurement. The voidage will be correct at the two end points. However, at all points in between these two calibration points, the measured values of inter-electrode capacitances or pixel values will depend on the distribution of the dielectric materials inside the sensor.

Simple image reconstruction techniques assume that the electric field is unchanged by the presence of varying dielectric materials inside the sensor. This means that to interpret the concentration of material from the permittivity map the use of a capacitance model is required. Such models would not be necessary if the full field were calculated based on the actual permittivity distribution. Yand and Byars [2] present two models based on simplified cases.

The simplest case assumes that the effective permittivity of the mixture can be obtained simply by summing the effects of the two components. This is known as the parallel capacitance model and corresponds to the case where there are effectively continuous bands of each dielectric material between the electrodes of the sensor. The parallel capacitance model tends to be valid for densely packed materials, such as liquids, or powdered/granular materials in dense-phase processes.

An alternative model is required for the situation where the higher permittivity material is present in dilute quantities in the mixture. This situation occurs, for example, in lean-phase fluidised beds or pneumatic conveying applications. The model which fits this situation is the series capacitance model, where we assume that the effective permittivity of a mixture of two materials can be found by assuming that the two materials act as two capacitors connected in series.

Many real flows do not fit these simplified models, and a model for a homogeneous mixture of small spheres developed by Maxwell in the 19th century has good general applicability [3], [4]. Using the Maxwell model the concentration of the denser phase of a two phase mixture (x) is given by equation 1.

$$x = K_{en}(2 + k)/(3 + K_{en}.(k - 1)), \qquad (1)$$

where k is the ratio K_H / K_L of the higher and lower relative permittivities of the two materials used for calibration. Note that if a particulate solid has been used for calibration then the relative permittivity is that of the bulk material, not the pure solid. Unless otherwise stated the Maxwell model has been used in deriving the results presented here.

FLOW ANALYSIS FROM IMAGES

By cross-correlating pixels or groups of pixels between one plane and a second axially separated plane, transit times and hence velocities can be measured. These measurements are effectively being taken as spatial averages over cylinders or cones along the sensor [5], [6].

Hunt et al [5] describe how the flow may be split up into contiguous zones for flowrate analysis and Figure 3 shows four examples of such zone maps. The leftmost image in the figure shows a zone map which would be suitable for horizontal two-component flow, the next one for annular flows, and the two right-hand zone maps are suitable for general flow measurement. Although we use fixed geometry

zones for the results presented here of simple uni-axial flows, such zones may be dynamically defined in more complex situations based on the flow structure itself [6].

Figure 5 shows a typical data screen for the passage of a plastic sphere dropped under gravity. The top plot shows concentration (left hand axis) against time for plane 1 (in green) and plane 2 (in red) for one particular zone – in this case the central one as highlighted on the zone map in the centre of the screen. The right hand axis indicates velocity in cm/s and refers to the blue line. In this case the structure is a sphere which cannot change shape, but the green and red vertical dotted lines indicate how particular structures may be identified for analysis. The lower left graph shows the result of the cross-correlation of the concentration signals from the two planes. The velocity at each point in time within each zone is calculated by correlating the instantaneous concentration of one plane with the same zone in the other plane. The result is plotted as a second graph with axes in cm/second on the left hand side of the graph. The correlation process is described mathematically as:

$$R_i(\tau) = \lim_{T\to\infty} \frac{1}{T} \int_0^T C_{1,i}(t) C_{2,i}(t+\tau)\, dt \qquad (2)$$

where $C_{1,i}(t)$ and $C_{2,i}(t)$ are the instantaneous concentrations in zone i in plane 1 and 2 respectively. Although mathematically the correlation is described for the averaging time T approaching infinity, in practice the velocity will fluctuate over some much shorter time scale and the user will need to set the window T at some suitable value appropriate to the particular length and velocity scales in the flow and the sensor geometry.

The resulting correlogram has a clearly discernible peak if the flow structures are coherent over the sensor length and contains information about the time domain statistics of the flow – primarily convection and dispersion. The simplest assumption is that the time delay at the peak of the correlogram corresponds to the transit time of flow structures between the two planes. The peak may be found by the greatest single value, centre of area or polynomial fitting. For many flows polynomial fitting gives the most consistent results though all the other techniques are available in the software. The time window used for the correlation process needs to be shaped in some way to minimize artefacts caused by sharp-edged windows. This shaping is known as *apodization* and various apodization functions are programmed into Flowan – the results presented here use the common *Hanning* window, which is a smooth bell shape.

If $\tau_i(t)$ is the time delay at the correlogram peak for zone i at each frame at time t, then the transit velocity is given by:

$$V_i(t) = S / \tau_i(t) \qquad (3)$$

where S is the separation distance between the centre of the sensor electrode planes. The peak of the correlogram in this instance is at a time delay of 0.067 seconds, corresponding to the transit time of the sphere between the two planes, and clearly seen on the concentration graph. The two images in the lower right of the screen show the images at the time of the cursor – shown as a vertical dotted black line at 2.465 seconds.

The sphere is passing through the sensor at about 200cm/s and accelerating under gravity – as indicated by the fact that the red curve is compressed in time compared to the green. Images from plane 1 at 5 ms intervals are shown in Figure6, starting at the top left and progressing left to right, top to bottom. Each image is a concentration map of solids distribution where red is a concentration of 1, and blue 0. To better understand the way the sphere is 'cut' by the images Figure 7 shows the approximate position of the sphere for the top left, middle and bottom right images of Figure 6.

The images may also be projected into isometric views, with an example shown in Figure 8. The sphere (shown as the contour 50% of solids) appears somewhat elongated – this is because the transit time has been used to calculate the velocity, and the concentration information is taken from plane 1. The sphere is in fact accelerating so the transit velocity between the two planes is higher than the actual velocity at plane 1, thus distorting the axial direction of the plot. At constant velocity the sphere would indeed appear spherical.

At 200 to 300 fps, with separation between the planes of the order of 0.1m, the measurements have a good resolution for velocities up to 10m/s.

VOLUME AND MASS ESTIMATION

By integrating over specified time periods around flow structures of interest it is possible to measure the volume of individual large particles or clusters of particles and by calibrating mass per unit length of the sensor, these measurements may be expressed directly as particle or cluster mass [8].

From the data screen shown in Figure 5, we have the concentration and velocity in every zone of the flow. The volumetric flow per zone is given by:

$$q_i(t) = V_i(t).C_i(t).A_i.\Delta t \qquad (4)$$

where Δt is the time interval between successive frames and A_i is cross-sectional area of each zone. $C_i(t)$ is in this case taken as the average of $C_{1,i}(t)$ and $C_{2,i}(t)$. The total volume flowing between time t_1 and t_2 can then be calculated as:

$$Q = \sum_{t=t_1,t_2} \sum_{i=1,n} q_i(t) \qquad (5)$$

The concentrations $C_{1,i}(t)$ and $C_{2,i}(t)$ are instantaneous averages over a volume corresponding to A_i x L_s where L_s is the sensor electrode length. The velocity $V_i(t)$ is an average over a volume A_i x (L_s + S) and also a time average over the correlation window T. The volumetric flowrate $q_i(t)$ is an average over the volume A_i x (L_s + S) and also a rolling average over T updated at each time frame Δt, q is often expressed in industrial situations as a 1 second value. The flow volume Q is integrated over the time period between time t_1 and t_2 and may be visualised as the equivalent to volume measurement through filling a tank over a time period.

In the case of a solid object Q is the volume of the object., in the case of a continuos flow of dispersed solids it is the volume of solids in a defined period of time. For the specific sphere shown in Figure 5 the estimation of volume is 61cm^3 ± 0.5cm^3, compared to the true value of 60cm^3 ± 1cm^3 estimated from linear measurement. The mass is estimated from ECT

using the bulk density of the solids as 35g ± 0.5g, compared to the true value of 35.2g ± 0.1g estimated by weighing.

GRAVITY DROP EXPERIMENTS

Two sets of simple gravity drop experiments are reported here to show the performance of the technique. Firstly a variety of plastic solid objects were dropped through the sensor. Figure 9 shows the objects which varied from 3g to 150g. The results of the experiments are shown in Figure 10.

The second set of experiments used the gravity drop rig described in Hunt et al [5] and shown in Figure 11. Known quantities of various types of solids were allowed to drop through the sensor, and the integrated measurements of flow as described here were then compared to the weighed quantity collected. Figure 12 shows these results.

It is clear from Figures 10 and 12 that for a variety of solid objects and solids flows the technique gives good estimation of total mass.

DENSE-PHASE CONVEYING

In pilot-scale flows the technique also performs well. Jaworski and Dyakowski [9] report experiments using ECT in a 50mm diameter recirculating rig circulating blown solids. In Figure 13 we show an example from those experiments, using our technique to analyze the data. In the figure the upper plot shows concentration and velocity from ECT. Lower pictures show image planes corresponding to axial locations on high-speed video stills. On the left of the Figure the green concentration line (plane 1) is in advance of the red line (plane 2), while on the right hand side of the figure the red line is in advance of the green indicating that the flow is in the opposite direction. Plane 1 is above plane 2, so the left hand structure is moving downwards, while the right-hand structure is moving upwards. The image planes are shown alongside stills from a high-speed video of the flow. The downflow appears disperse from the video still (the moving image shows downward 'roping' of the solids) while the image planes show that the solids are in fact only around a part of the periphery of the pipe. The upflow appears as a 'slug' of solds in the video, which the image planes show to be not fully filling the pipe. The time data shown is for the zone on the right-hand side of the image plane, other zones show different patterns of up and down flow – in these complex flows, although the overall flowrate is upwards there is a lot of flow reversal, and the flow mat be up and down simultaneously in the same cross section.

The velocity plot is in blue for upward and mauve for downward flow, showing the solid slug accelerating from about 2m/s to 3m/s, while the downward roping is at about 1m/s. Integrating the upflow and downflow separately gives a volume of 252 cm^3 passing down and a volume of 3392 cm^3 passing upwards over this 2 second period.

It is not possible to compare the volumetric measurements estimated from ECT in these flows with the reference integrated mass flows from the rig's weigh tank. The flows are highly periodic, and the ECT measurements were only taken over a short period of time. The slug volumes are quite consistent with rough calculations made from visual evidence, but the uncertainty of measurement in such flows will have to be evaluated by further experiments.

CONCLUSIONS

We have demonstrated that ECT can be used to measure the concentration, velocity and volume of solids and flows of solid particles. In simple flows the measurements are accurate to within a few percent, in complex flows the measurements are consistent with other estimates. ECT has great potential as a flow visualization tool and as a quantitative measurement of flowrate in two-phase flows.

ACKNOWLEDGMENTS

We gratefully acknowledge the support of the UK Department of Trade and Industry through a SMART award to Tomoflow Ltd.

REFERENCES

[1] Byars M. and Pendleton J.D., 2003. A new high-speed control interface for an electrical capacitance tomography system, 3rd World Congress on Industrial Process Tomography, Banff, Canada, 3-5 September 2003.

[2] Yang W.Q. and Byars M., 1999. An improved Normalisation Approach for Electrical Capacitance Tomography, 1st World Congress on Industrial Process Tomography, Buxton, UK, 14-17 April 1999.

[3] Wu Y., Li H., Wang M. and Williams R.A. 2003, A study on the characterization of air-water two-phase vertical flow by using electrical resistance imaging. 3rd World Congress on Industrial Process Tomography, Banff, Canada.

[4] Tortora P.R., Ceccio S.L., Schultz W.W., O'Hern T.J., Torczynski J.R. and Trujillo S.M. 2003, An electrical-impedance tomography system for collecting validation-quality data from gas-solid flows. 3rd World Congress on Industrial Process Tomography, Banff, Canada.

[5] Hunt A., Pendleton J.D., and White RB, 2003. A Novel Tomographic Flow Analysis System. 3rd World Congress on Industrial Process Tomography, Banff, Canada, 3-5 September 2003.

[6] Hunt A., Pendleton J.D. and Byars M. 2004. Visualisation of two-phase gas-liquid pipe flows using electrical capacitance tomography. ESDA2004-58396

[7] Dyakowski T., Mosorov V., Sankowski D., Seaton M., Mazurkiewicz Ł., Grudzień K and Jaworski A. 2003, Virtual channel concept for measuring solids mass flow rate. 3rd World Congress on Industrial Process Tomography, Banff, Canada.

[8] Hunt A. 2003, Mass measurement of moving objects using electrical capacitance tomography. Force and Hardness Group Annual Meeting, National Physical Laboratory, Teddington UK. 13 May 2003.

[9] .Jaworski A.J. and Dyakowski T. 2001. Tomographic measurements of solids mass flow in dense pneumatic conveying. What do we need to know about the flow phyics? 2nd World Congress on Industrial Process Tomography, Hannover, Germany, 29-31 August 2001.

FIGURES

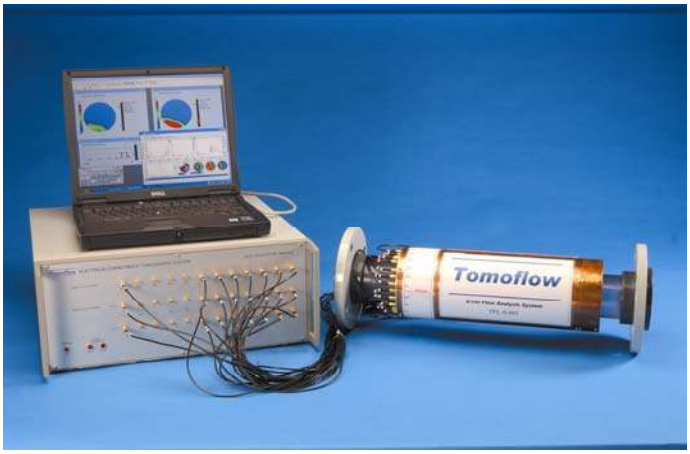

Figure 1. Tomoflow R100 ECT Flow Analysis System

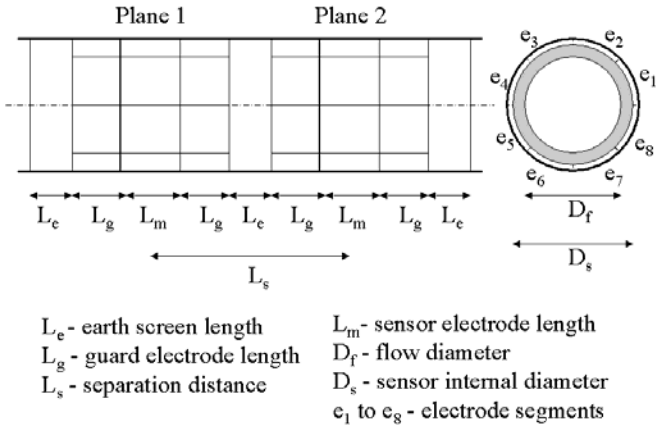

Figure 2. Electrode arrangement inside sensor

Figure 3. Photograph of sensor showing internal electrodes and connectors

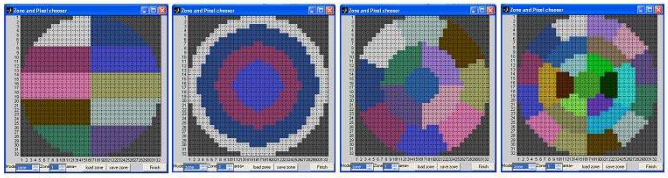

Figure 4. Examples of zone maps

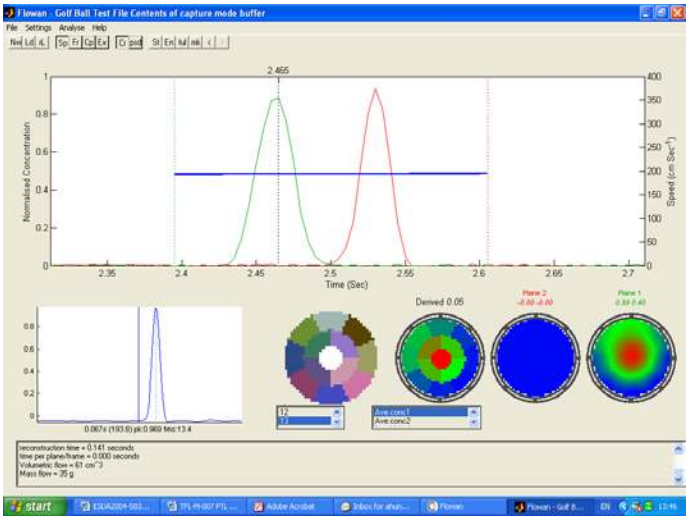

Figure 5. Data screen for plastic sphere dropped under gravity

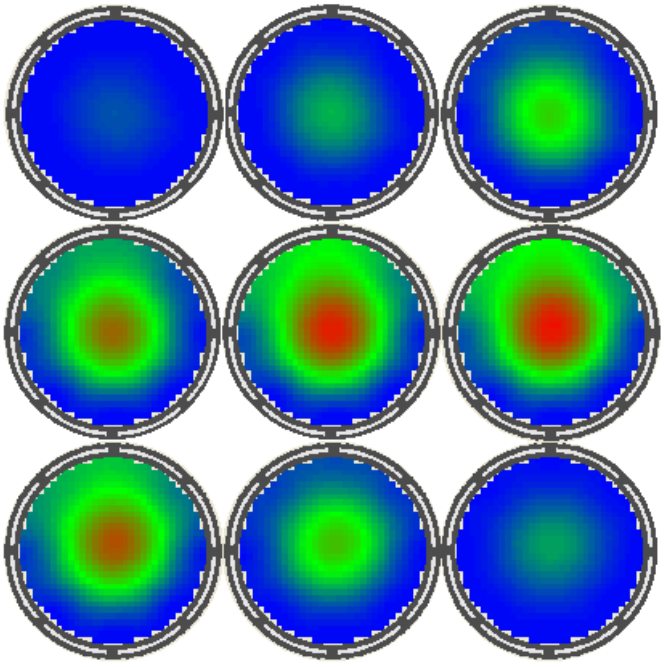

Figure 6. Images of plastic sphere at 5ms intervals

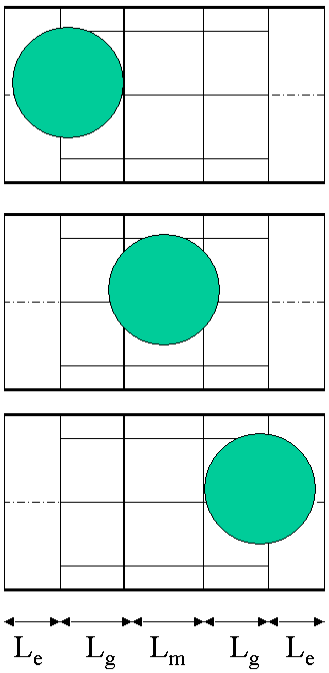

Figure 7. Approximate position of plastic sphere corresponding to top left, centre and bottom right images in Figure 6

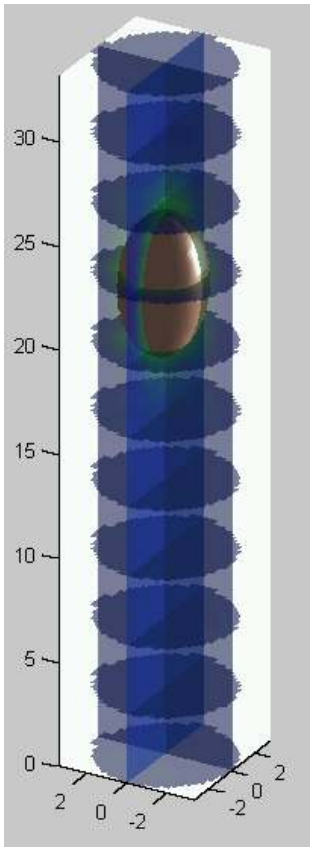

Figure 8. Plastic sphere reconstructed from images with 3D contour plot at 50% concentration together with axial and radial concentration 'slices'

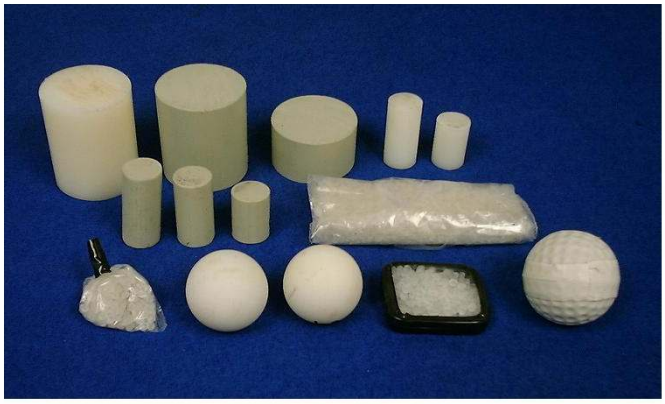

Figure 9. Various solids used for mass measurement tests

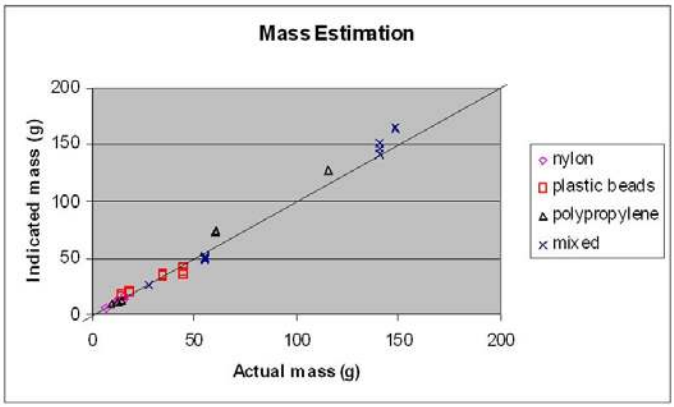

Figure 10. Mass estimation from ECT

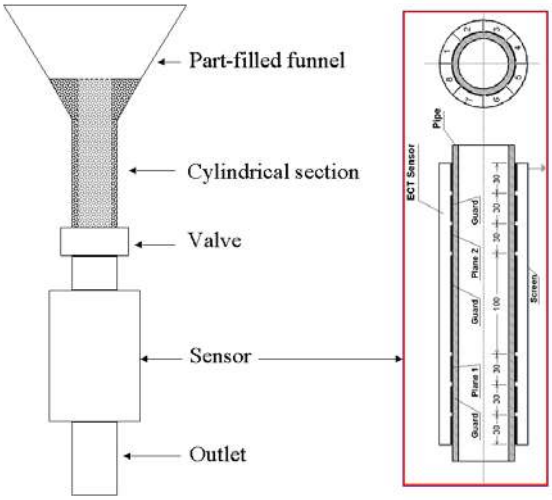

Figure 11. Simple gravity-drop rig

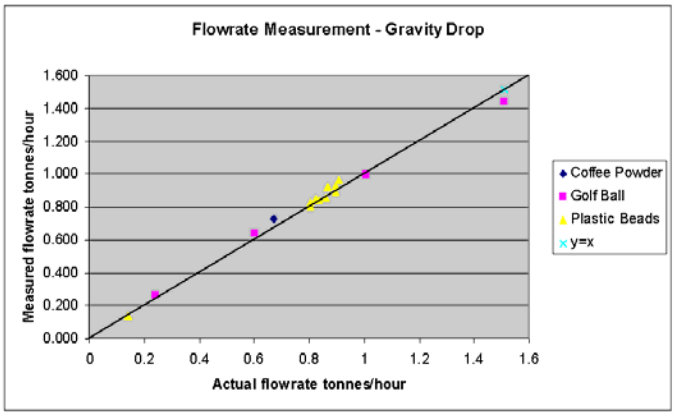

Figure 12. Mass flowrate estimation using ECT

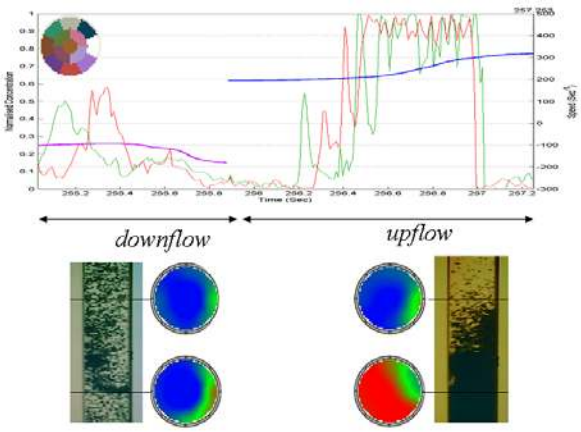

Figure 13. Vertical upflow of solids. Upper plot shows concentration and velocity from ECT. Lower pictures show image planes corresponding to axial locations on high-speed video stills. Downflow has a volume of 252 cm^3, upflow is 3392 cm^3